

Differential Flatness-Based Observer Design for a PEM Fuel Cell Using Adaptive-Gain Sliding Mode Differentiators

Jianxing Liu, Salah Laghrouche, and Maxime Wack

Laboratoire IRTES, Université de Technologie de Belfort-Montbéliard, France.
jiang-xing.Liu@utbm.fr; salah.laghrouche@utbm.fr; maxime.wack@utbm.fr

Abstract—In this paper, we propose a differential flatness-based observer for a PEM fuel cell air-feed system. The proposed observer uses the measurements of supply manifold air pressure and compressor mass flow rate in order to estimate the oxygen partial pressure, nitrogen partial pressure and the compressor speed. An adaptive-gain Second Order Sliding Mode differentiator based on super-twisting algorithm is designed to estimate the time derivatives of the system outputs when the boundary of higher time derivative is *unknown*. Then, the states are estimated based on these values. The objective is to minimize the number of embedded sensors in order to get a precise and economic solution. The feasibility and effectiveness of the proposed approach is demonstrated through simulation results obtained from a nonlinear fuel cell system.

I. INTRODUCTION

Fuel Cells are electrochemical devices that convert the chemical energy of a reaction between hydrogen and oxygen into electricity and are widely regarded as a potential alternative stationary and mobile power source [1]. A typical fuel cell power system consists of several auxiliary components, such as hydrogen supply system to the anode; air supply system to the cathode; deionized water serving as coolant in the stack cooling channel and deionized water supply to the humidifier to humidify the hydrogen and the air flows [2].

A major problem in the fuel cell stack is oxygen starvation when the load changes rapidly. The oxygen depleted from the fuel cell cathode needs to be regulated fast and efficiently to avoid oxygen starvation and extend the life of the stack [3]. Several model-based control approaches have been proposed for the fuel cell power systems. Linear control methods based on model linearization such as linear quadratic regulator (LQR), proportional integral (PI) plus static feed-forward (FF) controller are proposed in [2]. However, given the highly nonlinear nature of fuel cell stack, it is natural to apply model-based nonlinear robust control strategies that directly compensate for system nonlinearity without requiring a linear approximation, guarantee good performance in a wider range than those achieved based on model linearization. Sliding mode technique is known for its insensitivity to external disturbances, high accuracy and finite time convergence [4], [5]. Second Order Sliding Mode (SOSM) control strategy based on super-twisting algorithm is proposed in [6], [7]. In [6], the controller is used to control a permanent-magnet synchronous motor (PMSM) that drives a volumetric compressor (twin screw) to feed the fuel cell with air. The controller proposed in [7] guarantees maximization of

power generation efficiency. The control objective is to avoid oxygen starvation which is equivalent to regulate the oxygen excess ratio to its desired value. However, to evaluate the performance of the controller, it is important to calculate the value of oxygen excess ratio which requires the information of cathode pressure, supply manifold pressure and stack current. The extra use of sensor results high cost and low accuracy, therefore, the efficient observer design is of great interest.

Several observers have been designed for the fuel cell systems, such as adaptive observer [8], [9], Unscented Kalman Filter (UKF) [10], [11], linear parameter varying (LPV) observer [12]. There have been only a few studies of the applications of estimation with sliding mode technique to fuel cell systems. A sliding mode observer proposed in [13] has been used to estimate the state of charge for lithium battery. In the work of [14], Levant's differentiator [15], [16] is employed to estimate the parameters in an uncertain nonlinear system. In this paper, we combine the differential flatness theory [17] with the adaptive-gain sliding mode differentiator [18], [19], in order to design the observer for a fuel cell system. Differential flatness theory [17] allows an alternate representation of the system. One major property of differential flatness is that, the state and input variables can be directly expressed, without integrating any differential equation, in terms of the flat output and a finite number of its derivatives. Flatness-based approach has been applied in some nonlinear systems [20], [21]. An adaptive-gain sliding mode differentiator based on the work of [15], [16], [18], [19] is used to estimate the time derivatives of output variables in finite time. The proposed observer estimates the partial pressures of oxygen and nitrogen and the compressor speed from the measurements of supply manifold air pressure and compressor mass flow rate. The main *contributions* in this paper are:

- There is no a-priori requirements on the bound of the higher time derivative of the system outputs;
- There are no need the extra sensors for measuring the partial pressures of oxygen and nitrogen, and the compressor speed.

The rest of the paper is divided as follows: The mathematical model of the PEMFC dynamics is described in Section II. In Section III, the method of flatness-based observer is designed. In Section V, simulation results are presented.

Finally, conclusions are made in Section VI.

II. NONLINEAR FUEL CELL MODEL

In this Section, the nonlinear dynamic model of the fuel cell is present [3]. This model has four states, $x = [p_{O_2} \ p_{N_2} \ \omega_{cp} \ p_{sm}]^T$, where p_{O_2} is the oxygen pressure (Pa), p_{N_2} is the nitrogen pressure (Pa), ω_{cp} is the compressor speed (r/min) and p_{sm} is the supply manifold pressure (Pa). The cathode pressure is then calculated using Dalton's law of partial pressures ($p_{ca} = p_{O_2} + p_{N_2} + p_{sat}$).

The oxygen and the nitrogen pressures are calculated from the ideal gas law,

$$\begin{aligned} \frac{dp_{O_2}}{dt} &= \frac{RT_{st}}{M_{O_2}V_{ca}}(W_{O_2,in} - W_{O_2,out} - W_{O_2,react}), \\ \frac{dp_{N_2}}{dt} &= \frac{RT_{st}}{M_{N_2}V_{ca}}(W_{N_2,in} - W_{N_2,out}), \end{aligned} \quad (1)$$

where V_{ca} is the lumped volume of cathode, R is the universal gas constant, and M_{O_2}, M_{N_2} are the molar mass of oxygen and nitrogen, respectively.

The inlet mass flow rates of oxygen and the nitrogen $W_{O_2,in}, W_{N_2,in}$ can be calculated from the inlet cathode flow $W_{ca,in}$,

$$\begin{aligned} W_{O_2,in} &= x_{O_2}W_{ca,in}, \\ W_{N_2,in} &= (1 - x_{O_2})W_{ca,in}, \end{aligned} \quad (2)$$

where x_{O_2} is the oxygen mass fraction of the inlet air, and the mass flow rate entering the cathode $W_{ca,in}$,

$$W_{ca,in} = \frac{1}{1 + \omega_{atm}} k_{ca,in}(p_{sm} - p_{ca}), \quad (3)$$

where $\omega_{atm} = \frac{M_v}{M_{a,ca,in}} \frac{\phi_{ca} p_{sat}(T_{atm})}{p_{atm} - \phi_{ca} p_{sat}(T_{atm})}$ is the humidity ratio, $M_v, M_{a,ca,in}$ are the molar mass of vapor and air respectively, ϕ_{ca} is the relative humidity at ambient conditions, $p_{sat}(T_{atm})$ is the saturation pressure at ambient temperature, p_{atm} is the atmospheric pressure and $k_{ca,in}$ is the cathode inlet orifice constant.

The outlet mass flow rates of oxygen and nitrogen $W_{O_2,out}, W_{N_2,out}$ are calculated from the mass fraction of oxygen and nitrogen in the stack after the reaction,

$$\begin{aligned} W_{O_2,out} &= \frac{M_{O_2}p_{O_2}}{M_{O_2}p_{O_2} + M_{N_2}p_{N_2} + M_v p_{sat}} W_{ca,out}, \\ W_{N_2,out} &= \frac{M_{N_2}p_{N_2}}{M_{O_2}p_{O_2} + M_{N_2}p_{N_2} + M_v p_{sat}} W_{ca,out}, \end{aligned} \quad (4)$$

The flow rate at the cathode exit $W_{ca,out}$ is calculated by the nozzle flow equation [2],

$$\begin{aligned} W_{ca,out} &= \frac{C_D A_T p_{ca}}{\sqrt{RT_{st}}} \left(\frac{p_{atm}}{p_{ca}} \right)^{\frac{1}{\gamma}}, \text{ if } \frac{p_{atm}}{p_{ca}} > \left(\frac{2}{\gamma + 1} \right)^{\frac{\gamma}{\gamma - 1}} \\ &\times \left\{ \frac{2\gamma}{\gamma - 1} \left[1 - \left(\frac{p_{atm}}{p_{ca}} \right)^{\frac{\gamma - 1}{\gamma}} \right] \right\}, \end{aligned} \quad (5)$$

and

$$W_{ca,out} = \frac{C_D A_T p_{ca}}{\sqrt{RT_{st}}} \gamma^{\frac{1}{2}} \left(\frac{2}{\gamma + 1} \right)^{\frac{\gamma}{2(\gamma - 1)}}, \text{ else} \quad (6)$$

where γ is the ratio of the specific heat capacities of the air (all the parameters can be found in [2]).

The mass flow rate of oxygen consumption $W_{O_2,react}$ is expressed as follows,

$$W_{O_2,react} = \frac{nI_{st}}{4F} M_{O_2}, \quad (7)$$

where n is the number of cells in the stack, F is the Faraday number and I_{st} is the stack current.

The compressor motor state is described with the rotational speed ω_{cp} ,

$$\frac{d\omega_{cp}}{dt} = \frac{1}{J_{cp}} (\tau_{cm} - \tau_{cp}), \quad (8)$$

where J_{cp} is the compressor motor inertia, τ_{cm} is the compressor motor torque input ($N \cdot m$) and τ_{cp} is the torque required to drive the compressor ($N \cdot m$).

$$\begin{aligned} \tau_{cm} &= \eta_{cm} \frac{k_t}{R_{cm}} (v_{cm} - k_v \omega_{cp}), \\ \tau_{cp} &= \frac{C_p}{\omega_{cp}} \frac{T_{atm}}{\eta_{cp}} \left[\left(\frac{p_{sm}}{p_{atm}} \right)^{\frac{\gamma - 1}{\gamma}} - 1 \right] W_{cp} \end{aligned} \quad (9)$$

where k_t, R_{cm} and k_v are motor constants, η_{cm} is the motor mechanical efficiency. C_p is the specific heat capacity of air and W_{cp} is the compressor mass flow rate.

The dynamics of the air pressure in the supply manifold depend on the compressor flow into the supply manifold W_{cp} (double screw compressor is considered $W_{cp} = Ax_3$), the flow out of the supply manifold into the cathode $W_{ca,in}$ and the compressor flow temperature T_{cp} ,

$$\frac{dp_{sm}}{dt} = \frac{RT_{cp}}{M_a V_{sm}} [W_{cp} - k_{ca,in}(p_{sm} - p_{ca})], \quad (10)$$

where V_{sm} is the supply manifold volume and T_{cp} is the temperature of the air leaving the compressor,

$$T_{cp} = T_{atm} + \frac{T_{atm}}{\eta_{cp}} \left[\left(\frac{p_{sm}}{p_{atm}} \right)^{\frac{\gamma - 1}{\gamma}} - 1 \right], \quad (11)$$

Then, the nonlinear state model based on equations (1,8,10),

$$\begin{cases} \dot{x}_1 = c_1(x_4 - x_1 - x_2 - c_2) - \frac{c_3 x_1 W_{ca,out}}{c_4 x_1 + c_5 x_2 + c_6} - c_7 \zeta, \\ \dot{x}_2 = c_8(x_4 - x_1 - x_2 - c_2) - \frac{c_3 x_2 W_{ca,out}}{c_4 x_1 + c_5 x_2 + c_6}, \\ \dot{x}_3 = -c_9 x_3 - c_{10} \left[\left(\frac{x_4}{c_{11}} \right)^{c_{12}} - 1 \right] + c_{13} u, \\ \dot{x}_4 = c_{14} \left[1 + c_{15} \left[\left(\frac{x_4}{c_{11}} \right)^{c_{12}} - 1 \right] \right] \\ \quad \times [W_{cp} - c_{16}(x_4 - x_1 - x_2 - c_2)], \end{cases} \quad (12)$$

where the constants c_1, c_2, \dots, c_{16} are defined in Appendix. The control input u is the motor quadratic current, the input ζ is the stack current (which is considered as external disturbance to the system).

The system output is defined by,

$$y = \begin{bmatrix} y_1 \\ y_2 \end{bmatrix} = \begin{bmatrix} p_{sm} \\ W_{cp} \end{bmatrix}, \quad (13)$$

The system performance is defined by oxygen excess ratio $\lambda_{O_2} = \frac{W_{O_2,in}}{W_{O_2,react}}$, which can be calculated as,

$$\lambda_{O_2} = \frac{c_{17}}{c_{18}\zeta}(p_{sm} - p_{ca}) = \frac{c_{17}}{c_{18}\zeta}(x_4 - x_1 - x_2 - c_2), \quad (14)$$

The control objective is to drive λ_{O_2} to its desired value $\lambda_{O_2}^*$. The controller system is decomposed into 2 parts: the external loop (λ_{O_2} controller) and the internal loop (ω_{cp} controller). The λ_{O_2} controller based on the reference value of $\lambda_{O_2}^*$ and its estimated value in order to generate the reference of compressor speed ω_{cp}^* . The ω_{cp} controller produces the control input u based on output of λ_{O_2} controller and its estimated value.

In the next Section, an adaptive-gain sliding mode differentiator observer is designed based on the property of differential flatness.

III. DIFFERENTIAL FLATNESS-BASED OBSERVER DESIGN

A. Brief Theory of Differential Flatness

A system is said to be flat if one can find a set of state variables, so-called the **flat outputs**, such that the system is algebraic over the differential field generated by the flat outputs and its derivatives [17]. Here, we consider general nonlinear systems of the form,

$$\begin{aligned} \dot{x} &= f(x, u), \\ x &= [x_1, x_2, \dots, x_n]^T, \quad x \in R^n \\ u &= [u_1, u_2, \dots, u_m]^T, \quad u \in R^m \end{aligned} \quad (15)$$

where x is the state variable, u is the vector of input (control) variables, and $(n, m) \in N$.

According to previous works, if the state variables x can be parameterized by output y and its derivatives, an autonomous dynamical system is said to be differentially flat and admits the flat output y

$$y = h(x) = [y_1, y_2, \dots, y_m]^T, \quad y \in R^m \quad (16)$$

with

$$y = \phi(x, u, \dot{u}, \dots, u^{(\alpha)}) \quad (17)$$

such that the state variable and control variable can be written as follows:

$$\begin{aligned} x &= \varphi(y, \dot{y}, \dots, y^{(\beta)}), \\ u &= \psi(y, \dot{y}, \dots, y^{(\beta+1)}) \end{aligned} \quad (18)$$

where α and β are the finite numbers of derivative.

B. Flatness-Based Observer Design

Consider the system (15,16). From the observability rank condition in [22], [23], if the following Jacobian matrix is full-ranked, the observability rank condition is achieved.

$$\mathcal{O} = \begin{bmatrix} dL_f^0(h_1) & \dots & dL_f^0(h_m) \\ \vdots & \ddots & \vdots \\ dL_f^{n-1}(h_1) & \dots & dL_f^{n-1}(h_m) \end{bmatrix}, \quad (19)$$

where $L_f h = \frac{\partial h}{\partial x} f$ is called the *Lie Derivative* of h with respect to f . The observability analysis of the system (12) is based on the system outputs (13) and the knowledge of the controller u . Then, one can get,

$$\text{rank}(\mathcal{O}) = n = 4, \quad (20)$$

The cathode pressure p_{ca} is denoted as a new variable $X = x_1 + x_2 + c_2$, the system (12) can be rewritten as flat form with the outputs (13),

$$\begin{aligned} X &= y_1 - \frac{y_2}{c_{16}} + \frac{\dot{y}_1}{c_{14}c_{16} \left[1 + c_{15} \left[\left(\frac{y_1}{c_{11}} \right)^{c_{12}} - 1 \right] \right]} \\ &= \varphi_1(y_1, \dot{y}_1, y_2), \end{aligned} \quad (21)$$

and

$$\begin{aligned} \dot{X} &= \dot{\varphi}_1 = \dot{y}_1 - \frac{\dot{y}_2}{c_{16}} + \frac{\ddot{y}_1}{c_{14}c_{16} \left[1 + c_{15} (y_1^{c_{12}} - 1) \right]} \\ &\quad - \frac{c_{15}c_{12}y_1^{(c_{12}+1)}}{c_{14}c_{16} \left[1 + c_{15} (y_1^{c_{12}} - 1) \right]^2} = \varphi_2(y_1, \dot{y}_1, \ddot{y}_1, \dot{y}_2), \end{aligned} \quad (22)$$

$$\begin{aligned} x_1 &= \frac{1}{c_4 - c_5} \left[\frac{c_3(\varphi_1 - c_2)W_{ca,out}}{(c_4 + c_8)(y_1 - \varphi_1) - \varphi_2 - c_7\xi} \right. \\ &\quad \left. + c_2c_5 - c_6 - c_5\varphi_1 \right] = \varphi_3(y_1, \dot{y}_1, \ddot{y}_1, y_2, \dot{y}_2), \end{aligned} \quad (23)$$

$$x_2 = X - x_1 - c_2 = \varphi_4(y_1, \dot{y}_1, \ddot{y}_1, y_2, \dot{y}_2), \quad (24)$$

$$x_3 = \frac{y_2}{A} = \varphi_5(y_2), \quad (25)$$

$$x_4 = y_1 = \varphi_6(y_1), \quad (26)$$

where $W_{ca,out}$ takes the form of (5,6) which is the function of variable X .

Remark 1: Considering that the the two outputs y_1 and y_2 are measurable, their first time and second time derivatives are estimated by employing an adaptive-gain sliding mode differentiator. In the work of [14], the estimation of parameters is obtained via Levant's differentiator [15], [16] based on the property of flat systems.

C. Adaptive-Gain Sliding Mode Differentiator

Let's recall a finite time convergent differentiator based on Super-Twisting (STW) algorithm [15]. Consider the following equation,

$$\begin{aligned} \dot{x}_1 &= -\lambda |x_1 - f(t)|^{\frac{1}{2}} \text{sign}(x_1 - f(t)) + x_2, \\ \dot{x}_2 &= -\alpha \text{sign}(x_1 - f(t)), \end{aligned} \quad (27)$$

where the second-order differentiable signal $f(t)$ is assumed to be bounded $|\dot{f}(t)| \leq L_2$, L_2 is a *known* positive constant. Then, the sufficient conditions for the finite time convergence of $e_1 = x_1 - f(t)$ and $e_2 = x_2 - \dot{f}(t)$ to zero:

$$\alpha > L_2, \quad \lambda^2 \geq 4L_2 \frac{\alpha + L_2}{\alpha - L_2}, \quad (28)$$

The main drawback of the above algorithm is the requirement of *known* boundary of $|\dot{f}(t)|$. However, in practical cases the boundary can not be easily obtained which requires

extensive experimentation in worst case conditions, and the obtained results may still remain inconclusive when considered from system to system. The adaptive-gain of STW algorithm is proposed to overcome this difficulty [24].

Theorem 1: Consider the system (27) under the following adaptation laws,

$$\begin{cases} \lambda(t) = 2\sqrt{L(t)} \\ \alpha(t) = 4L(t) \end{cases} \quad (29)$$

the adaptive law of the positive time varying function $L(t)$ is given by,

$$\dot{L}(t) = \begin{cases} k & \text{if } e_1 \neq 0 \\ 0 & \text{else} \end{cases} \quad (30)$$

where $k > 0$ is a positive design constant, and the initial value $L(0) > \frac{1}{4}$. Then for any initial conditions $x_1(0), x_2(0), e_1(t), e_2(t)$ will converge to zero in finite time.

Proof: Define the errors $e_1 = x_1 - f(t)$ and $e_2 = x_2 - \dot{f}(t)$. Then, the system (27) can be rewritten as follows,

$$\begin{cases} \dot{e}_1 = -\lambda(t)|e_1|^{\frac{1}{2}} \text{sign}(e_1) + e_2, \\ \dot{e}_2 = -\alpha(t)\text{sign}(e_1) + \ddot{f}(t). \end{cases} \quad (31)$$

where $|\ddot{f}(t)| \leq F$ where F is an *unknown* positive constant.

Considering the following Lyapunov function candidate for the system (31,29,30),

$$V(\zeta(t), t) = \frac{1}{L^2(t)} \underbrace{\zeta^T(t)P(t)\zeta(t)}_{V_0(t)} + \frac{1}{2}(L(t) - L^*)^2, \quad (32)$$

where

$$\zeta^T(t) = \begin{bmatrix} |e_1|^{\frac{1}{2}} \text{sign}(e_1) \\ e_2 \end{bmatrix}, P(t) = \begin{bmatrix} \alpha(t) + \frac{\lambda^2(t)}{2} & -\frac{\lambda(t)}{2} \\ -\frac{\lambda(t)}{2} & 1 \end{bmatrix} \quad (33)$$

Here L^* is a positive constant. System (31) can be rewritten as,

$$\dot{\zeta}(t) = \frac{1}{2|\zeta_1(t)|} A\zeta(t) + B\ddot{f}(t), \quad \zeta_1(t) = C\zeta(t). \quad (34)$$

where

$$A = \begin{bmatrix} -\lambda(t) & 1 \\ -2\alpha(t) & 0 \end{bmatrix}, \quad B = [0 \quad 1]^T, \quad C = [1 \quad 0]. \quad (35)$$

Taking the derivative of (32), we obtain

$$\dot{V}(t, \zeta) = \underbrace{\frac{d}{dt} \left(\frac{1}{L^2(t)} \zeta^T P \zeta \right)}_{\dot{V}_1} + \underbrace{\frac{d}{dt} \left(\frac{1}{2} (L(t) - L^*)^2 \right)}_{\dot{V}_2}. \quad (36)$$

The first component of (36) can be calculated as,

$$\dot{V}_1 = \underbrace{\zeta^T \frac{d}{dt} \left(\frac{P(t)}{L^2(t)} \right) \zeta}_{\dot{V}_{1a}} + \underbrace{\frac{1}{L^2(t)} \left(\dot{\zeta}^T P(t) \zeta + \zeta^T P(t) \dot{\zeta} \right)}_{\dot{V}_{1b}} \quad (37)$$

Substituting (30,33) into \dot{V}_{1a} ,

$$\dot{V}_{1a} = \zeta^T \underbrace{\begin{bmatrix} -6L^{-2}(t) & \frac{3}{2}L^{-\frac{5}{2}}(t) \\ \frac{3}{2}L^{-\frac{5}{2}}(t) & -2L^{-3}(t) \end{bmatrix}}_{\Upsilon(t)} \dot{L}(t) \zeta \quad (38)$$

since $\dot{L}(t) \geq 0$ and $L > 0$ for all the time. It can be shown that matrix $\Upsilon(t)$ is negative definite, i.e.

$$\dot{V}_{1a} \leq 0 \quad (39)$$

The term \dot{V}_{1b} in (37) is calculated as,

$$\dot{V}_{1b} \leq -\frac{1}{L^2(t)} \frac{1}{2|\zeta_1|} \zeta^T Q(t) \zeta. \quad (40)$$

where $A(t)^T P(t) + P(t) A(t) + 4(F)^2 C^T C + P(t) B B^T P(t) = -Q(t)$, From (35), the symmetric matrix $Q(t)$ is calculated as,

$$Q(t) = \begin{bmatrix} 8L^{\frac{3}{2}}(t) - L(t) - 4(F)^2 & L^{\frac{1}{2}}(t) \\ L^{\frac{1}{2}}(t) & 2L^{\frac{1}{2}}(t) - 1 \end{bmatrix}. \quad (41)$$

Then, (40) can be rewritten as,

$$\dot{V}_{1b} \leq -\frac{1}{L(t)} \frac{1}{2|\zeta_1|} \zeta^T \tilde{Q}(t) \zeta. \quad (42)$$

where

$$\tilde{Q}(t) = \begin{bmatrix} \frac{8L^{\frac{3}{2}}(t) - L(t) - 4(F)^2}{L(t)} & L^{-\frac{1}{2}}(t) \\ L^{-\frac{1}{2}}(t) & \frac{2L^{\frac{1}{2}}(t) - 1}{L(t)} \end{bmatrix}, \quad (43)$$

As $L(t) \geq L(0) > \frac{1}{4}$, we get $2L^{\frac{1}{2}}(t) - 1 > 0$. The matrix $\tilde{Q}(t)$ will be positive definite if

$$8L^{\frac{3}{2}}(t) - L(t) - \frac{L(t)}{2L^{\frac{1}{2}}(t) - 1} > 4(F)^2 \quad (44)$$

Since

$$\lambda_{\min}(P(t)) \|\zeta\|^2 \leq V_0(t) \leq \lambda_{\max}(P(t)) \|\zeta\|^2 \quad (45)$$

$$|\zeta_1| \leq \|\zeta\|_2 \leq \frac{V_0^{\frac{1}{2}}(t)}{\lambda_{\min}^{\frac{1}{2}}(P(t))}, \quad \|\zeta\|^2 \geq \frac{V_0(t)}{\lambda_{\max}(P(t))}$$

Considering Equation (42), we assume that Equation (44) holds (for the reason that the left part of (44) is increasing as $L(t)$ increases constantly), then it is easy to show that,

$$\dot{V}_{1b}(t) \leq -\frac{\eta}{L(t)} V_0^{\frac{1}{2}}. \quad (46)$$

where $\eta = \frac{\lambda_{\min}(Q(t))}{\lambda_{\max}^{\frac{1}{2}}(P(t))}$. It is assumed that the adaptive law of (30) makes $L(t)$ bounded (this assumption will be proved later). Then, there exists positive constant L^* such that $L(t) - L^* < 0$ for all the time.

Considering (46), Equation (36) can be rewritten as,

$$\begin{aligned} \dot{V}(t, \zeta) &\leq -\frac{\eta}{L(t)} V_0^{\frac{1}{2}} - \sqrt{2}k \frac{|L(t) - L^*|}{\sqrt{2}} \\ &\leq -\min\{\eta_2, \sqrt{2}k\} \left(\frac{V_0^{\frac{1}{2}}}{L(t)} + \frac{|L(t) - L^*|}{\sqrt{2}} \right) \\ &\leq -\bar{\eta} V^{\frac{1}{2}} \end{aligned} \quad (47)$$

with $\bar{\eta} = \min\{\eta, \sqrt{2k}\}$. As soon as inequality (44) is satisfied, the finite time convergence of e_1, e_2 to zero is guaranteed from any initial condition $\zeta(0)$, and the reaching time t_F can be easily estimated as

$$t_F \leq \frac{2V^{\frac{1}{2}}(0)}{\bar{\eta}}. \quad (48)$$

which proves the theorem. \blacksquare

From the Theorem 1, the estimates of $\dot{y}_1, \ddot{y}_1, \dot{y}_2$ can be obtained in finite time. Therefore, the system state variables can be estimated in finite time from the flat outputs y_1, y_2 .

IV. SIMULATION RESULTS

In this Section, we demonstrate the observer design process proposed in Section III based on the nonlinear dynamic model (12). The proposed method has been simulated in the Matlab/Simulink environment, the integration was carried out according to the Euler method, the sampling step being equal to the integration step $\tau = 10^{-4}$. The parameters for the simulation are shown in APPENDIX [2]. For the simulation purpose, the initial values are chosen as

$$x(0) = [1.0\text{bar} \quad 0.66\text{bar} \quad 1500\text{r/min} \quad 1.3\text{bar}]^T, \quad (49)$$

The system (12) is assumed to be well controlled where the controller used in the simulation is based on [25] which means the oxygen excess ratio is driven to its desired value, typically $\lambda_{O_2}^* = 2$.

The stack current shown in Fig. 1 consists of rapid variations between 100A and 400A, which is chosen from the work of [2].

Figs. (2,3,4) show that the state variables are well estimated based on the adaptive-gain STW sliding mode differentiator. Fig. (6) shows the efficacy of the proposed adaptive-gain STW algorithm.

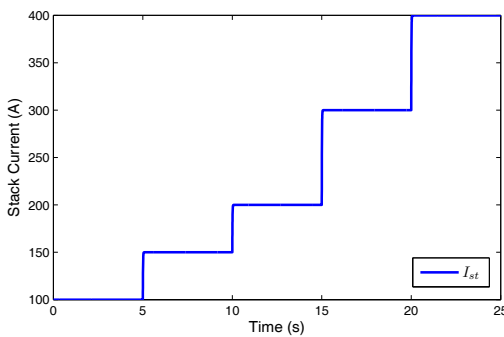


Fig. 1. Stack Current

V. CONCLUSIONS

Fuel cell technology presents numerous opportunities for nonlinear control applications. Observers are of great interest both for robust feedback controller design and sensor reduction. In this paper, an adaptive-gain sliding mode differentiator based on differential flatness for a PEM fuel cell system is designed. The state variables can be parameterized

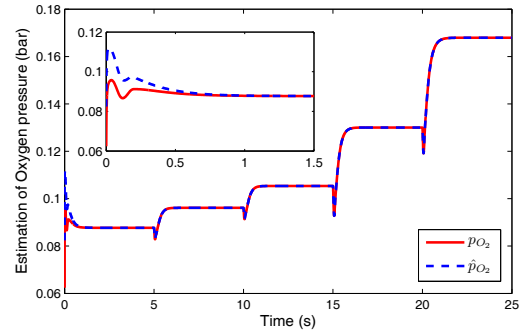


Fig. 2. Estimation of Oxygen pressure

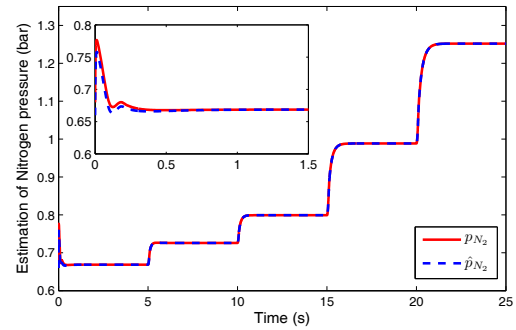


Fig. 3. Estimation of Nitrogen pressure

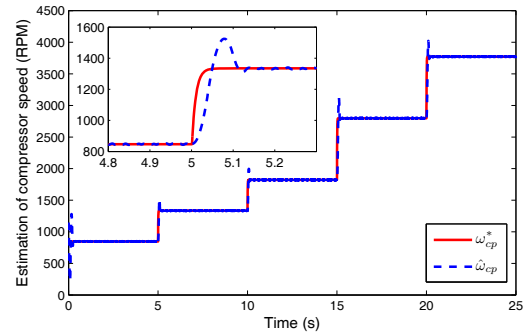


Fig. 4. Estimation of compressor speed

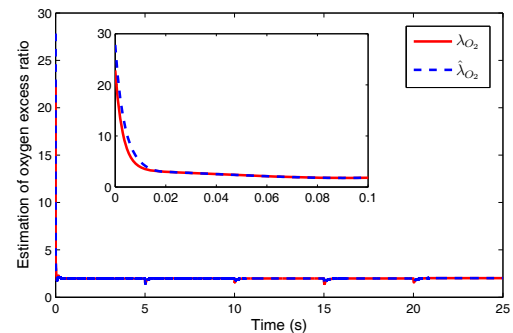


Fig. 5. Estimation of oxygen excess ratio

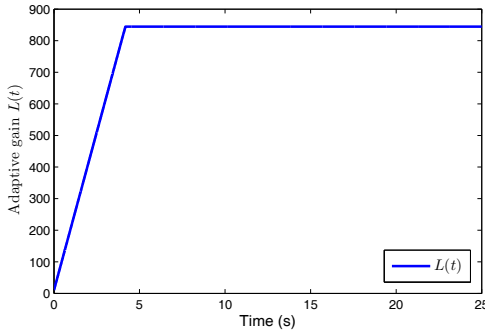


Fig. 6. Adaptive gain $L(t)$

as system's flat outputs and its time derivatives. These time derivatives of the outputs can be obtained from the proposed differentiator in finite time. The proposed observer estimates the partial pressures of oxygen and nitrogen, and compressor speed from the measurements of supply manifold air pressure and compressor mass flow rate. Simulation results show the feasibility and effectiveness of the proposed observer.

APPENDIX

$$\begin{aligned}
 c_1 &= \frac{\bar{R}T_{st}k_{ca,in}}{M_{O_2}V_{ca}} \left(\frac{x_{O_2,atm}}{1+\omega_{atm}} \right); & c_2 &= p_{sat} \\
 c_3 &= \frac{\bar{R}T_{st}}{V_{ca}}; & c_4 &= \frac{\bar{R}T_{st}n}{4V_{ca}F} \\
 c_8 &= \frac{\bar{R}T_{st}k_{ca,in}}{M_{N_2}V_{ca}} \left(\frac{1-x_{O_2,atm}}{1+\omega_{atm}} \right); \\
 c_9 &= \frac{\eta_{cm}k_t}{J_{cp}}; & c_{10} &= \frac{C_p T_{atm}}{J_{cp}\eta_{cp}} \\
 c_{11} &= p_{atm}; & c_{12} &= \frac{\gamma-1}{\gamma} \\
 c_{13} &= \frac{\eta_{cm}k_t}{J_{cp}}; & c_{14} &= \frac{\gamma \bar{R}T_{atm}}{M_{a,atm}V_{sm}} \\
 c_{15} &= \frac{1}{\eta_{cp}}; & c_{16} &= k_{ca,in} \\
 c_{17} &= \frac{C_D A_T}{\sqrt{\bar{R}T_{st}}} \sqrt{\frac{2\gamma}{\gamma-1}}; & c_{18} &= \frac{1}{\gamma} \\
 A &= \frac{1}{2\pi} \eta_{v-c} V_{cpr/tr} \rho_a; & c_{19} &= \left(\frac{2}{\gamma+1} \right)^{\frac{\gamma}{\gamma-1}} \\
 c_{20} &= \frac{C_D A_t}{\sqrt{\bar{R}T_{st}}} \gamma^{\frac{1}{2}} \left(\frac{2}{\gamma+1} \right)^{\frac{\gamma+1}{2(\gamma-1)}}.
 \end{aligned}$$

REFERENCES

- [1] L. Carrette, K. Friedrich, and U. Stimming, "Fuel Cells—Fundamentals and Applications," *Fuel cells*, vol. 1, no. 1, pp. 5–39, 2001.
- [2] J. Pukrushpan, A. Stefanopoulou, and H. Peng, *Control of Fuel Cell Power Systems: Principles, Modeling, Analysis and Feedback Design*. Springer, 2004.
- [3] —, "Control of Fuel Cell Breathing," *IEEE Control Systems*, vol. 24, no. 2, pp. 30–46, 2004.
- [4] V. Utkin, J. Gulder, and J. Shi, *Sliding Mode Control in Electro-Mechanical Systems*, ser. Automation and Control Engineering Series. Taylor & Francis Group, 2009.
- [5] S. Laghrouche, F. Plestan, and A. Glumineau, "Higher Order Sliding Mode Control Based on Integral Sliding Mode," *Automatica*, vol. 43, no. 3, pp. 531–537, 2007.
- [6] R. Talj, D. Hissel, R. Ortega, M. Becherif, and M. Hilaret, "Experimental Validation of a PEM Fuel-Cell Reduced-Order Model and a Moto-Compressor Higher Order Sliding-Mode Control," *IEEE Transactions on Industrial Electronics*, vol. 57, no. 6, pp. 1906–1913, 2010.
- [7] C. Kunusch, P. Puleston, M. Mayosky, and J. Riera, "Sliding Mode Strategy for PEM Fuel Cells Stacks Breathing Control Using a Super-Twisting Algorithm," *IEEE Transactions on Control Systems Technology*, vol. 17, no. 1, pp. 167–174, 2009.

- [8] M. Arcak, H. Görgün, L. M. Pedersen, and S. Varigonda, "A Nonlinear Observer Design for Fuel Cell Hydrogen Estimation," *IEEE Transactions on Control Systems Technology*, vol. 12, no. 1, pp. 101–110, 2004.
- [9] H. Görgün, F. Barbir, and M. Arcak, "A Voltage-Based Observer Design for Membrane Water Content in PEM Fuel Cells," in *Proceedings of the 2005 American Control Conference*. IEEE, 2005, pp. 4796–4801.
- [10] R. Vepa, "Adaptive State Estimation of a PEM Fuel Cell," *IEEE Transactions on Energy Conversion*, vol. 27, no. 2, pp. 457–467, 2012.
- [11] A. Murshed, B. Huang, and K. Nandakumar, "Estimation and Control of Solid Oxide Fuel Cell System," *Computers & Chemical Engineering*, vol. 34, no. 1, pp. 96–111, 2010.
- [12] S. De Lira, V. Puig, J. Quevedo, and A. Husar, "LPV Observer Design for PEM Fuel Cell System: Application to Fault Detection," *Journal of Power Sources*, vol. 196, no. 9, pp. 4298–4305, 2011.
- [13] I.-S. Kim, "The novel state of charge estimation method for lithium battery using sliding mode observer," *Journal of Power Sources*, vol. 163, no. 1, pp. 584–590, 2006.
- [14] M. Iqbal, A. Bhatti, S. Ayubi, and Q. Khan, "Robust Parameter Estimation of Nonlinear Systems Using Sliding-Mode Differentiator Observer," *IEEE Transactions on Industrial Electronics*, vol. 58, no. 2, pp. 680–689, 2011.
- [15] A. Levant, "Robust Exact Differentiation Via Sliding Mode Technique," *Automatica*, vol. 34, no. 3, pp. 379–384, 1998.
- [16] —, "Higher-Order Sliding Modes, Differentiation and Output-Feedback Control," *International Journal of Control*, vol. 76, no. 9–10, pp. 924–941, 2003.
- [17] M. Fliess, J. Lévine, P. Martin, and P. Rouchon, "Flatness and Defect of Non-Linear Systems: Introductory Theory and Examples," *International Journal of Control*, vol. 61, no. 6, pp. 1327–1361, 1995.
- [18] S. Yuri, T. Mohammed, and P. Franck, "A Novel Adaptive-Gain Super-twisting Sliding Mode Controller: Methodology and Application," *Automatica*, vol. 48, no. 5, pp. 759–769, 2012.
- [19] J. A. Moreno and M. Osorio, "A Lyapunov Approach to Second-Order Sliding Mode Controllers and Observers," in *47th IEEE Conference on Decision and Control (CDC)*. IEEE, 2008, pp. 2856–2861.
- [20] M. Danzer, J. Wilhelm, H. Aschemann, and E. Hofer, "Model-Based Control of Cathode Pressure and Oxygen Excess Ratio of a PEM Fuel Cell System," *Journal of Power Sources*, vol. 176, no. 2, pp. 515–522, 2008.
- [21] A. Houari, H. Renaudineau, J.-P. Martin, S. Pierfederici, and F. Meibody-Tabar, "Flatness-Based Control of Three-Phase Inverter With Output LC Filter," *IEEE Transactions on Industrial Electronics*, vol. 59, no. 7, pp. 2890–2897, 2012.
- [22] G. Besançon, *Nonlinear Observers and Applications*. Springer Verlag, 2007, vol. 363.
- [23] A. Isidori, *Nonlinear Control Systems*. Springer Verlag, 1995, vol. 1.
- [24] "Oscillatory failure case detection for aircraft using an adaptive sliding mode differentiator scheme."
- [25] I. Matraji, S. Laghrouche, S. Jemei, and M. Wack, "Robust Control of the PEM Fuel Cell Air-Feed System Via Sub-Optimal Second Order Sliding Mode," *Applied Energy*, vol. 104, pp. 945–957, 2013.